**Supporting Information**

*for*

# Quadruply B←N-Fused Dibenzo-azaacene with High Electron Affinity and High Electron Mobility

Yang Min,[†,§] Chuandong Dou,[†,*] Dan Liu,[‡,§] Huanli Dong[‡,*] and Jun Liu[†,*]

[†]*State Key Laboratory of Polymer Physics and Chemistry, Changchun Institute of Applied Chemistry, Chinese Academy of Sciences, Changchun 130022, P. R. China.*
[‡]*Beijing National Laboratory for Molecular Science, Key Laboratory of Organic Solids, Institute of Chemistry, Chinese Academy of Sciences, Beijing 100190, P. R. China.*
[§]*University of Chinese Academy of Sciences, Beijing 100049, P. R. China.*
E-mail: chuandong.dou@ciac.ac.cn; dhl522@iccas.ac.cn; liujun@ciac.ac.cn.

## *Contents*

## 1. Experimental details

**General.** $^{1}H$ and $^{13}C$ NMR spectra were obtained using a Bruker AV-400 (400 MHz for $^{1}H$ and 100 MHz for $^{13}C$) spectrometer in *d*-DMSO, $CDCl_3$ and $C_6D_6$ at 25 ℃. $^{11}B$ NMR spectra were measured with a Bruker AV III HD-500 spectrometer in $CDCl_3$ at 25 ℃. Chemical shifts are reported in $\delta$ ppm using *d*-DMSO (2.50 ppm), $CHCl_3$ (7.26 ppm) and $C_6H_6$ (7.16 ppm) for $^{1}H$ NMR, as well as using *d*-DMSO (39.52 ppm), $CDCl_3$ (77.16 ppm) and $C_6D_6$ (128.06 ppm) for $^{13}C$ NMR. For $^{11}B$ NMR, $BF_3 \cdot Et_2O$ was used as an external standard. Elemental analysis was conducted on a VarioEL elemental analyzer. Thermal analysis was performed on a Perkin-Elmer 7 instrument at a heating rate of 10 ℃ $min^{-1}$ under nitrogen flow. Absorption spectra were measured with a Shimadzu UV-3600 spectrometer using spectral grade solvents. Cyclic voltammetry (CV) was performed on an CHI660a electrochemical workstation using $Bu_4NClO_4$ (0.1 M) as electrolyte at a scan rate of 50 mV $s^{-1}$. The CV cell has a glassy carbon electrode, a Pt wire counter electrode, and a standard calomel reference electrode. The measurement was carried out under an argon atmosphene in $CH_2Cl_2$ (0.4 mM). The redox potentials were calibrated with ferrocene as an internal standard. The highest occupied molecular orbital (HOMO) and lowest unoccupied molecular orbital (LUMO) energy levels were calculated based on the equations: $E_{HOMO}/E_{LUMO} = -(4.80 + E_{pa}^{ox1}/E_{1/2}^{red1})$ eV. Atomic force microscopy (AFM) was performed with a SPA300HV (Seiko Instruments, Inc., Japan) in tapping mode. Polarized optical microscopy and scanning electron microscopy were performed using Carl Zeiss Microlmaging GmbH Axio Imager A2m and XL-30 ESEM FEG Scanning Electron Microscope FEI COMPANY™, respectively. Transmission electron microscopy (TEM) and selected-area electron diffraction (SEAD) were performed using a JEOL JEM-1011 transmission electron microscope operated at 100 kV. The grazing incidence X-ray diffraction (GI-XRD) data was obtained on a Bruker D8 Discover reflector (Cu Kα, $\lambda$ = 1.54056 Å) under 40 kV and 40 mA tube current. The scanning speed is 3 s per step with 0.1 ° step size ($2\theta$). The measurements were conducted in a scanning interval of $2\theta$ between 2 ° and 30 °.

**Materials and reagents.** All reactions were performed under an argon atmosphere, unless stated otherwise. Commercially available solvents and reagents were used without further purification unless otherwise mentioned. Dry toluene and $CH_2Cl_2$ were distilled via standard methods.

## 2. Syntheses and characterizations

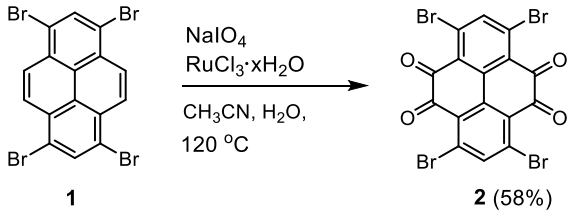


**1** **2** (58%)

**1,3,6,8-tetrabromopyrene-4,5,9,10-tetraone (2)**: In a 250 mL glass vessel equipped with J. Young valve, 1,3,6,8-tetrabromopyrene **1** (1.35 g, 2.61 mmol), $NaIO_4$ (5.30 g, 24.8 mmol) and $RuCl_3{\cdot}xH_2O$ (54 mg) were placed and $CH_3CN$ (60 mL) and $H_2O$ (13.5 mL) were added. The mixture was stirred at 120 $^oC$ for 15 h. After cooling down, the organic solvent was removed under reduced pressure and then $H_2O$ was added to the mixture. The mixture was filtered and the obtained solid was washed using $H_2O$, $CH_3OH$ and ether to give the target **2** in 58% yield. $^1H$ NMR (400 MHz, *d*-DMSO, 25 $^oC$): $\delta$ (ppm) 8.42 (s, 1H). $^{13}C$ NMR(100 MHz, *d*-DMSO, 25 $^oC$): $\delta$ (ppm) 177.05, 142.02, 136.62, 128.36, 127.80. Anal. Calcd for $C_{16}H_2Br_4O_4$: C, 33.26; H, 0.35; Br, 55.32; O, 11.08. Found: C, 33.15; H, 0.40.

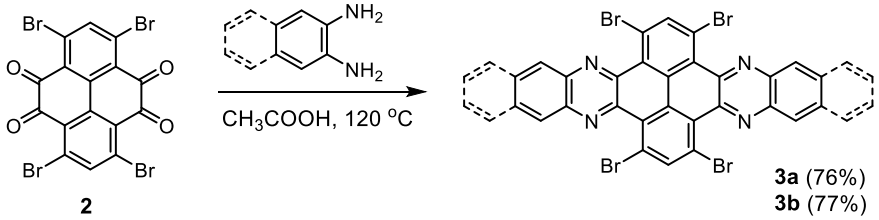


**2** **3a** (76%) **3b** (77%)

**1,3,10,12-tetrabromoquinoxalino[2',3':9,10]phenanthro[4,5-abc]phenazine (3a)**: 1,3,6,8-tetrabromopyrene-4,5,9,10-tetraone **2** (281 mg, 0.49 mmol) and benzene-1,2-diamine (110 mg, 1.01 mmol) were placed in a three-necked flask, followed by adding acetic acid (50 mL). The mixture was stirred at 120 $^oC$ for 9 h. After cooling down, the acetic acid was removed and the mixture was washed using $H_2O$ and then $CH_3OH$. The obtained target **3a** was used for the next step without further purification. Yield: 266 mg, 76%.

**1,3,12,14-tetrabromobenzo[i]benzo[6',7']quinoxalino[2',3':9,10]phenanthro[4,5-abc]phenazine (3b)**: 1,3,6,8-tetrabromopyrene-4,5,9,10-tetraone **2** (880 mg, 1.52 mmol) and naphthalene-2,3-diamine (506 mg, 3.20 mmol) were placed in a three-necked flask, followed by adding acetic acid (200 mL). The mixture was stirred at 120 $^oC$ for 20 h. After cooling down, the acetic acid was removed and the mixture was washed using $H_2O$, $CH_3OH$ and $CHCl_3$. The obtained target **3b** was used for the next step without further purification. Yield: 968 mg, 77%.

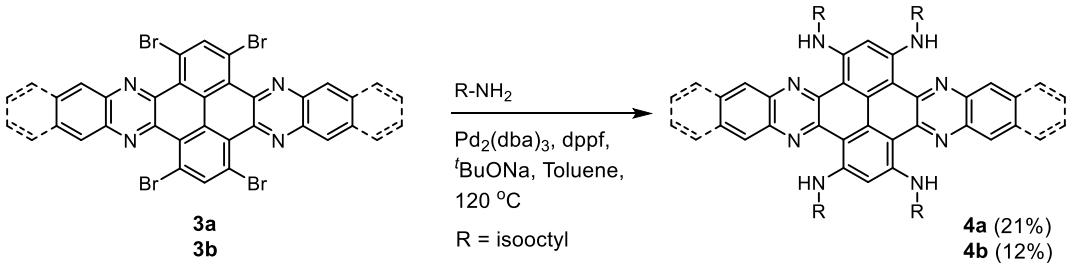


**N1,N3,N10,N12-tetrakis(2-ethylhexyl)quinoxalino[2',3':9,10]phenanthro[4,5-abc]phenazine-1,3,10,12-tetraamine (4a)**: Under argon, **3a** (150 mg, 0.21 mmol), $Pd_2(dba)_3$ (11.5 mg, 0.013 mmol), 1,1'-bis(diphenylphosphino)ferrocene (dppf) (28 mg, 0.051 mmol) and sodium *tert*-butoxide (320 mg, 3.33 mmol) were placed in a three-necked flask. Dried toluene (80 mL) and 2-ethylhexyl-amine (430 mg, 3.33 mmol) were then added. The mixture was stirred at 120 °C for 15 h. After cooling down, the mixture was extracted using water and $CH_2Cl_2$. The organic phase was dried over anhydrous $Na_2SO_4$, filtered and concentrated under reduced pressure. The crude product was purified by silica gel column chromatography with $CH_2Cl_2$:hexane = 1:2 as eluent to give **4a**. Yield: 40 mg, 21%. $^1$H NMR (400 MHz, $C_6D_6$, 25 °C): $\delta$ (ppm) 12.86 (t, $J$ = 4.0 Hz, 2H), 8.0 (m, 2H), 7.42 (m, 2H), 6.39 (s, 1H), 3.47 (m, 4H), 1.96 (m, 2H), 1.84−1.62 (m, 8H), 1.49−1.37 (m, 8H), 1.07 (t, $J$ = 4.0 Hz, 6H), 0.95 (t, $J$ = 8.0 Hz, 6H). $^{13}$C NMR(100 MHz, $C_6D_6$, 25 °C): $\delta$ (ppm) 153.80, 146.55, 137.92, 135.80, 126.97, 126.73, 103.44, 90.38, 46.98, 39.65, 32.41, 29.74, 25.48, 23.68, 14.46, 11.42. Anal. Calcd for $C_{60}H_{82}N_8$: C, 78.73; H, 9.03; N, 12.24. Found: C, 78.53; H, 9.15; N, 12.35.

**N1,N3,N12,N14-tetrakis(2-ethylhexyl)benzo[i]benzo[6',7']quinoxalino[2',3':9,10]phenanthro[4,5-abc]phenazine-1,3,12,14-tetraamine (4b)**: Under argon, **3b** (631 mg, 0.77 mmol), $Pd_2(dba)_3$ (42 mg, 0.046 mmol), 1,1'-bis(diphenylphosphino)ferrocene (dppf) (102 mg, 0.18 mmol) and sodium *tert*-butoxide (1.18 g, 12.3 mmol) were placed in a three-necked flask. Dried toluene (100 mL) and 2-ethylhexyl-amine (1.30 mg, 10 mmol) were then added. The mixture was stirred at 120 °C for 17 h. After cooling down, the mixture was extracted using water and $CH_2Cl_2$. The organic phase was dried over anhydrous $Na_2SO_4$, filtered and concentrated under reduced pressure. The crude product was purified by silica gel column chromatography with $CH_2Cl_2$:hexane = 1:1.5 as eluent to give **4b**. Yield: 76 mg, 12%. $^1$H NMR (400 MHz, $C_6D_6$, 25 °C): $\delta$ (ppm) 13.03 (t, $J$ = 2.0 Hz, 2H), 8.32 (s, 2H), 7.95 (m, 2H), 7.26 (m, 2H), 6.18 (s, 1H), 3.42 (m, 4H), 1.96−1.40 (m, 18H), 1.13 (t, $J$ = 8.0 Hz, 6H), 0.99 (t, $J$ = 4.0 Hz, 6H). $^{13}$C NMR(100 MHz, $C_6D_6$, 25 °C): $\delta$ (ppm) 154.12, 147.12, 136.18,

135.59, 133.28, 125.22, 123.37, 103.98, 90.05, 47.35, 39.58, 32.29, 29.72, 25.30, 23.81, 14.55, 11.43. Anal. Calcd for $C_{68}H_{86}N_8$: C, 80.43; H, 8.54; N, 11.03. Found: C, 80.32; H, 8.62; N, 11.01.

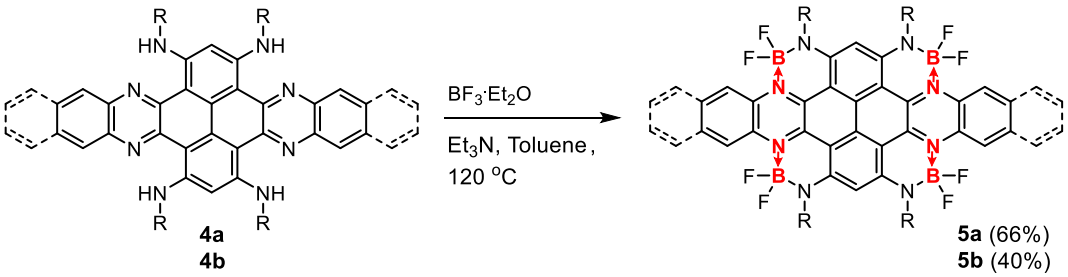


**1,8,10,17-tetrakis(2-ethylhexyl)-2,2,7,7,11,11,16,16-octafluoro-1,2,7,8,10,11,16,17-octahydro-1,2al4,6bl4,8,10,11al4,15bl4,17-octaaza-2l4,7l4,11l4,16l4-tetraboradibenzo[d,o]ovalene (5a):** Under argon, $BF_3{\cdot}Et_2O$ solution (2.89 mL) was added to a solution of **4a** (40 mg, 0.044 mmol) and $Et_3N$ (0.74 mL) in dry toluene (20 mL). The mixture was stirred at 120 ℃ for 6 h with the color changing into green. After removing the solvents, the solid was dispersed into methanol, followed by filtration. The obtained solid was purified by silica gel column chromatography ($CH_2Cl_2$:hexane = 1:1) to give **5a** in 66% yield (32 mg). $^1$H NMR (400 MHz, $CDCl_3$, 25 $^o$C): $\delta$ (ppm) 9.03 (m, 2H), 7.82 (m, 2H), 6.65 (s, 1H), 3.84 (d, $J$ = 4.0 Hz, 4H), 2.12 (m, 2H), 1.52−1.25 (m, 16H), 0.94−0.86 (m, 12H). $^{13}$C NMR(100 MHz, $CDCl_3$, 25 $^o$C): $\delta$ (ppm) 151.66, 137.08, 132.71, 132.05, 130.87, 124.09, 104.34, 93.97, 49.41, 36.86, 30.87, 28.83, 24.04, 23.34, 14.25, 10.74. $^{11}$B NMR (128 MHz, $CDCl_3$, 25 ℃): $\delta$ 2.55. Anal. Calcd for $C_{60}H_{78}B_4F_8N_8$: C, 65.13; H, 7.11; B, 3.91; F, 13.74; N, 10.13. Found: C, 65.23; H, 7.03; N, 10.21. High-resolution MALDI-TOF MS, Calcd for $C_{60}H_{78}B_4F_7N_8$: 1087.6610 (M−F), found 1087.6728.

**1,10,12,21-tetrakis(2-ethylhexyl)-2,2,9,9,13,13,20,20-octafluoro-1,2,9,10,12,13,20,21-octahydro-1,2al4,8bl4,10,12,13al4,19bl4,21-octaaza-2l4,9l4,13l4,20l4-tetraboradinaphtho[2,3-d:2',3'-o]ovalene (5b):** Under argon, $BF_3{\cdot}Et_2O$ solution (3.49 mL) was added to a solution of **4b** (37 mg, 0.036 mmol) and $Et_3N$ (0.88 mL) in dry toluene (20 mL). The mixture was stirred at 120 ℃ for 8 h with the color changing into green. After removing the solvents, the solid was dispersed into methanol, followed by filtration. The obtained solid was purified by silica gel column chromatography ($CHCl_3$:hexane = 2:1) to give **5b** in 40% yield (18 mg). $^1$H NMR (400 MHz, $CDCl_3$, 25 $^o$C): $\delta$ (ppm) 9.58 (s, 2H), 8.16 (m, 2H), 7.69 (m, 2H), 6.58 (s, 1H), 3.86 (d, $J$ = 4.0 Hz, 4H), 2.12 (m, 2H), 1.54−1.25 (m, 16H), 0.96−0.86 (m, 12H). $^{13}$C NMR(100 MHz, $CDCl_3$, 25 $^o$C): $\delta$ (ppm) 151.81, 137.45, 133.68, 131.89, 129.07, 128.90, 128.84, 122.56, 101.99, 93.90, 49.43, 36.98, 30.90, 28.85,

24.0, 23.42, 14.26, 10.78. $^{11}$B NMR (128 MHz, $CDCl_3$, 25 ℃): $\delta$ 2.34. Anal. Calcd for $C_{68}H_{82}B_4F_8N_8$: C, 67.69; H, 6.85; B, 3.58; F, 12.60; N, 9.29. Found: C, 67.58; H, 6.96; N, 9.19. High-resolution MALDI-TOF MS, Calcd for $C_{68}H_{82}B_4F_7N_8$: 1087.6923 (M−F), found 1187.6774.

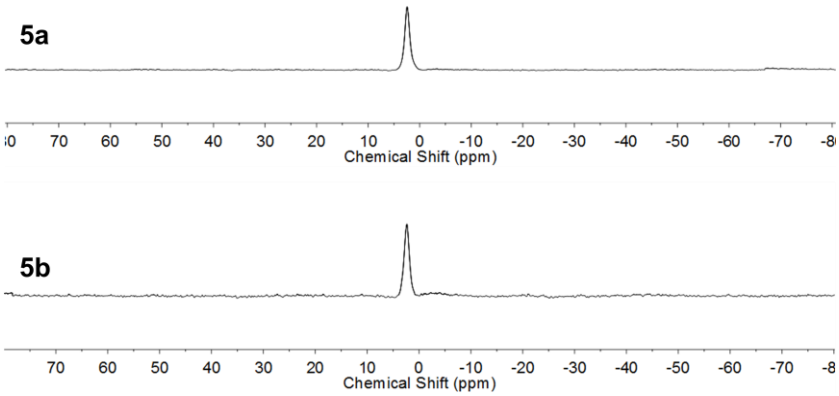


**Figure S1.** $^{11}$B NMR spectra of **5a** and **5b** in $CDCl_3$ at 25 ℃.

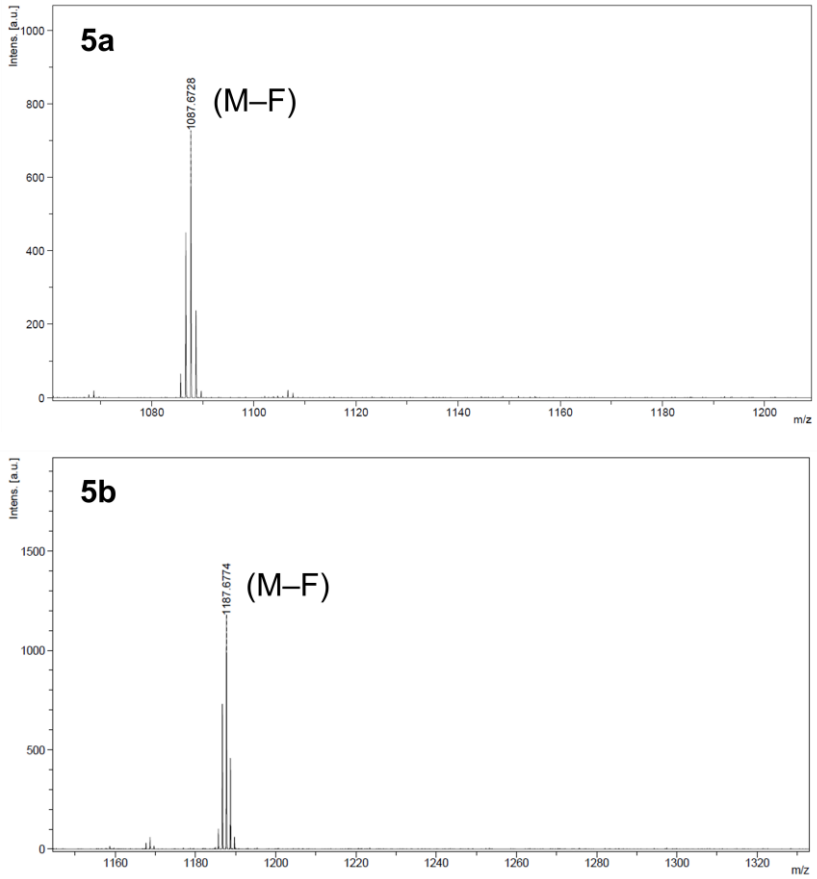


**Figure S2.** High-resolution MALDI-TOF MS spectra of **5a** and **5b**.

## 3. Thermal properties

Thermogravimetric analysis (TGA) measurements indicate that the thermal decomposition temperature ($T_d$) at 5% weight loss is 250 $^{o}$C for **5a** and 306 $^{o}$C for **5b**, respectively. **5b** shows a weight loss of 7.8% at 313 $^{o}$C in TGA curve, which is ascribed to the release of two $BF_2$ groups (theoretical value: 8.0%).

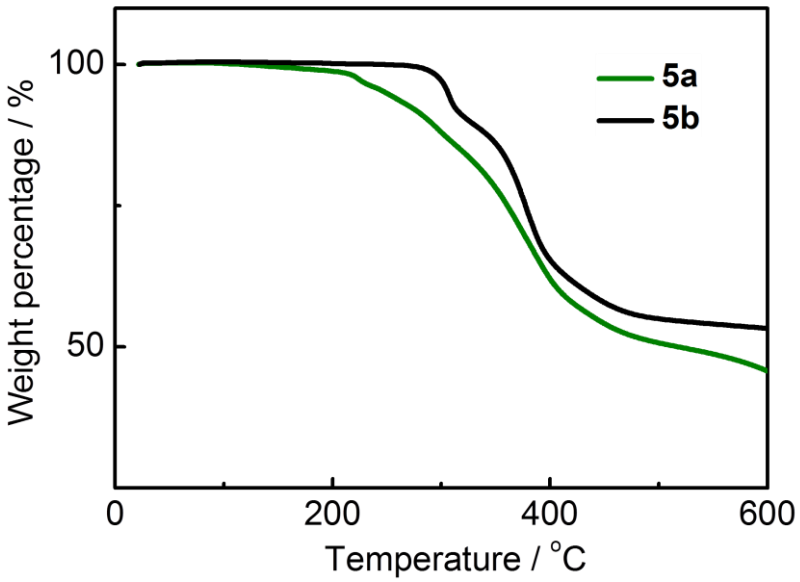


**Figure S3.** TGA curves of **5a** and **5b**.

**4. Geometry optimizations**

The geometry optimizations of **5a-Me** and **5b-Me**, as well as **5a-CC** and **5b-CC** were performed using Gaussian 09 program at the B3LYP/6-31G(d,p) level of theory.[1] **5a-Me** and **5b-Me** are the model compounds of **5a** and **5b** with methyl group replacing isooctyl chain. The C−C-containing polyarenes **5a-CC** and **5b-CC** are the analogues of **5a** and **5b**, which use the four C−C covalent bonds to replace the B←N units.

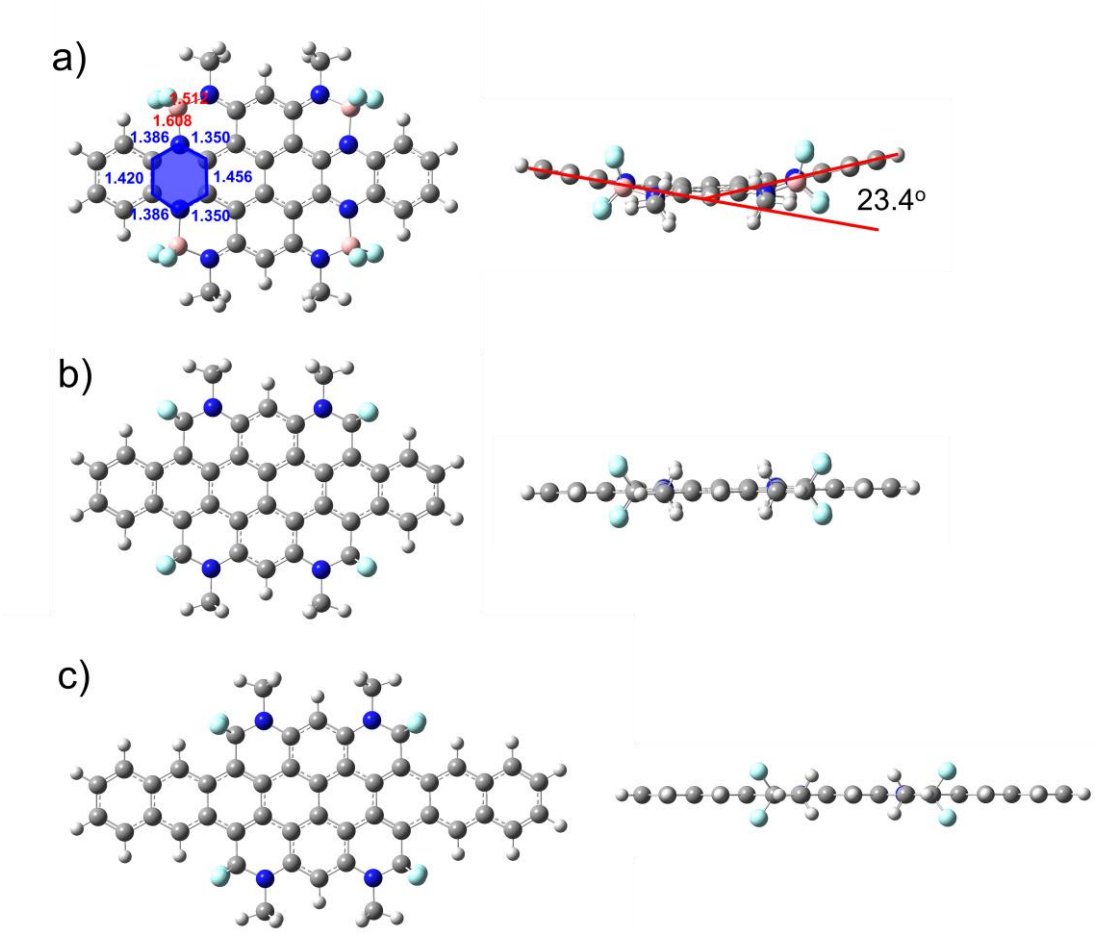


**Figure S4.** The optimized structures of a) **5a-Me**, b) **5a-CC** and c) **5b-CC** calculated at the B3LYP/6-31G(d,p) level of theory. The B←N-containing polyarenes exhibit the curved configurations, whereas the C−C-containing polyarenes show the fully planar configurations. It is suggested that the overcrowded B←N units can significantly impact on the molecular configurations.

**Table S1.** Coordinates of the optimized structure for **5a-Me** at the B3LYP/6-31G(d,p) level.

| atom | x | y | z |
|---|---|---|---|
| C | 0.00002400 | -3.52902200 | -0.45260700 |
| C | 1.22485200 | -2.86920900 | -0.33637300 |
| C | 1.23513500 | -1.42789600 | -0.15909200 |
| C | 0.00000400 | -0.72653600 | -0.13558800 |
| C | -1.23511200 | -1.42792200 | -0.15900400 |
| C | -1.22480600 | -2.86924400 | -0.33621600 |
| C | 2.46787600 | -0.72818800 | -0.03072700 |
| C | -0.00000700 | 0.72653600 | -0.13559200 |
| C | 1.23510900 | 1.42792300 | -0.15902300 |
| C | 2.46786300 | 0.72823300 | -0.03065500 |
| C | 1.22480300 | 2.86924300 | -0.33624500 |
| C | -0.00002900 | 3.52902100 | -0.45262400 |
| C | -1.22485500 | 2.86920900 | -0.33637500 |
| C | -1.23513800 | 1.42789600 | -0.15909100 |
| C | -2.46787800 | 0.72818900 | -0.03071500 |
| C | -2.46786400 | -0.72823100 | -0.03063500 |
| H | -0.00003800 | 4.59853000 | -0.57124000 |
| C | 4.82617900 | 0.70986000 | 0.30593000 |
| C | 4.82619700 | -0.70980900 | 0.30578400 |
| C | -4.82619600 | 0.70981000 | 0.30581600 |
| C | -4.82617600 | -0.70985900 | 0.30595800 |
| C | 6.03515600 | 1.40418500 | 0.55782500 |
| H | 6.04064300 | 2.48114500 | 0.57503500 |
| C | 6.03519600 | -1.40417200 | 0.55745700 |
| H | 6.04070600 | -2.48113800 | 0.57437400 |
| C | 7.19579500 | -0.70391600 | 0.79726200 |
| C | 7.19577100 | 0.70389600 | 0.79746500 |
| C | -6.03515000 | -1.40418900 | 0.55785200 |
| H | -6.04063400 | -2.48114900 | 0.57504600 |
| C | -6.03519500 | 1.40416700 | 0.55750500 |
| H | -6.04070800 | 2.48113200 | 0.57443200 |
| C | -7.19579000 | 0.70390700 | 0.79731500 |
| C | -7.19576400 | -0.70390500 | 0.79750400 |
| N | -3.63958000 | 1.38977300 | 0.08017000 |
| N | -3.63954600 | -1.38983000 | 0.08037900 |
| N | 3.63954700 | 1.38983200 | 0.08034900 |

| | | | |
|---|---|---|---|
| N | 3.63957900 | -1.38977200 | 0.08015100 |
| N | -2.38563400 | 3.53785900 | -0.42317000 |
| B | -3.73212800 | 2.99259800 | -0.00308700 |
| F | -4.10090000 | 3.45788800 | 1.25484100 |
| F | -4.69259500 | 3.31921800 | -0.95380400 |
| C | -2.38392700 | 4.97116700 | -0.70986800 |
| H | -1.94509000 | 5.55113500 | 0.11137900 |
| H | -1.82667700 | 5.18334900 | -1.62860200 |
| H | -3.41472100 | 5.28879300 | -0.85523900 |
| H | 0.00003200 | -4.59853200 | -0.57121900 |
| N | -2.38557500 | -3.53793400 | -0.42283700 |
| B | -3.73203600 | -2.99267700 | -0.00264500 |
| C | -2.38385300 | -4.97125500 | -0.70947500 |
| H | -1.82674100 | -5.18345500 | -1.62828900 |
| H | -1.94485900 | -5.55116800 | 0.11172600 |
| H | -3.41465700 | -5.28893000 | -0.85466800 |
| F | -4.10064500 | -3.45780100 | 1.25539000 |
| F | -4.69258500 | -3.31948900 | -0.95321400 |
| N | 2.38563200 | -3.53785900 | -0.42317600 |
| N | 2.38557100 | 3.53793100 | -0.42289000 |
| C | 2.38392400 | -4.97116800 | -0.70987200 |
| H | 1.94509300 | -5.55113500 | 0.11137800 |
| H | 1.82666700 | -5.18335100 | -1.62860200 |
| H | 3.41471700 | -5.28879200 | -0.85525000 |
| C | 2.38384800 | 4.97124900 | -0.70954200 |
| H | 1.82671500 | 5.18344200 | -1.62834500 |
| H | 1.94487600 | 5.55117200 | 0.11166400 |
| H | 3.41465000 | 5.28891900 | -0.85476200 |
| F | 4.10089200 | -3.45787200 | 1.25484400 |
| F | 4.69259900 | -3.31922600 | -0.95379900 |
| F | 4.10067900 | 3.45784400 | 1.25529300 |
| F | 4.69256600 | 3.31946200 | -0.95332200 |
| B | 3.73212500 | -2.99259700 | -0.00309100 |
| B | 3.73204000 | 2.99267900 | -0.00272000 |
| H | 8.11334000 | -1.24808800 | 0.99576000 |
| H | 8.11329700 | 1.24803900 | 0.99612800 |
| H | -8.11328700 | -1.24805200 | 0.99616700 |
| H | -8.11333300 | 1.24807500 | 0.99582500 |

**Table S2.** Coordinates of the optimized structure for **5b-Me** at the B3LYP/6-31G(d,p) level.

| atom | x | y | z |
|---|---|---|---|
| C | -0.00005000 | 3.52751100 | -0.64533200 |
| C | -1.22445600 | 2.86853900 | -0.52160400 |
| C | -1.23461800 | 1.42809800 | -0.33288200 |
| C | -0.00001200 | 0.72764300 | -0.30751000 |
| C | 1.23456100 | 1.42816500 | -0.33255600 |
| C | 1.22436100 | 2.86864400 | -0.52099700 |
| C | -2.46845900 | 0.73092600 | -0.19270100 |
| C | 0.00001400 | -0.72762000 | -0.30752100 |
| C | -1.23455500 | -1.42813600 | -0.33265600 |
| C | -2.46841100 | -0.73099100 | -0.19245000 |
| C | -1.22436600 | -2.86860400 | -0.52118100 |
| C | 0.00004500 | -3.52746800 | -0.64551500 |
| C | 1.22445100 | -2.86852600 | -0.52155600 |
| C | 1.23461400 | -1.42808100 | -0.33285900 |
| C | 2.46845200 | -0.73090900 | -0.19265300 |
| C | 2.46842300 | 0.73101100 | -0.19243200 |
| H | 0.00006300 | -4.59594000 | -0.77317000 |
| C | -4.82585900 | -0.71682700 | 0.16997200 |
| C | -4.82594000 | 0.71673100 | 0.16953800 |
| C | 4.82593700 | -0.71673900 | 0.16957100 |
| C | 4.82590900 | 0.71681600 | 0.16981300 |
| C | -6.01110100 | -1.40473200 | 0.43599100 |
| H | -6.01701700 | -2.48248100 | 0.45702000 |
| C | -6.01130900 | 1.40463100 | 0.43502100 |
| H | -6.01743600 | 2.48239100 | 0.45531300 |
| C | -7.20307000 | 0.71867800 | 0.69834400 |
| C | -7.20296000 | -0.71878500 | 0.69887200 |
| C | 6.01121400 | 1.40470100 | 0.43561500 |
| H | 6.01721900 | 2.48245400 | 0.45638100 |
| C | 6.01127000 | -1.40466200 | 0.43514900 |
| H | 6.01729900 | -2.48241900 | 0.45569800 |
| C | 7.20307600 | -0.71873100 | 0.69831400 |
| C | 7.20304700 | 0.71873200 | 0.69855800 |
| N | 3.63477200 | -1.39374100 | -0.07584500 |
| N | 3.63471200 | 1.39385500 | -0.07536100 |
| N | -3.63467400 | -1.39385400 | -0.07529300 |

| | | | |
|---|---|---|---|
| N | -3.63479400 | 1.39374900 | -0.07593500 |
| N | 2.38544000 | -3.53545800 | -0.61240800 |
| B | 3.72870100 | -2.99402300 | -0.17492600 |
| F | 4.08440400 | -3.47666300 | 1.08111200 |
| F | 4.69755900 | -3.31333300 | -1.11948900 |
| C | 2.38532300 | -4.96571500 | -0.91276700 |
| H | 1.94597900 | -5.55403400 | -0.09767600 |
| H | 1.82921700 | -5.16953000 | -1.83408900 |
| H | 3.41673100 | -5.28057600 | -1.05983700 |
| H | -0.00006200 | 4.59600000 | -0.77285100 |
| N | 2.38532900 | 3.53569200 | -0.61128300 |
| B | 3.72844800 | 2.99420200 | -0.17342000 |
| C | 2.38520700 | 4.96599100 | -0.91143200 |
| H | 1.82931300 | 5.16991100 | -1.83285700 |
| H | 1.94563200 | 5.55417000 | -0.09636300 |
| H | 3.41663800 | 5.28091700 | -1.05819900 |
| F | 4.08353400 | 3.47606100 | 1.08307500 |
| F | 4.69767100 | 3.31427900 | -1.11737700 |
| C | 8.42075000 | 1.40963800 | 0.97757900 |
| H | 8.41507200 | 2.49561600 | 0.97685900 |
| C | 9.57149900 | 0.71270800 | 1.23908400 |
| H | 10.49420100 | 1.24495700 | 1.44915600 |
| C | 8.42080600 | -1.40968200 | 0.97710900 |
| H | 8.41517100 | -2.49566100 | 0.97602300 |
| C | 9.57152700 | -0.71279400 | 1.23884700 |
| H | 10.49425100 | -1.24507700 | 1.44873800 |
| C | -8.42083100 | 1.40961300 | 0.97703700 |
| H | -8.41526300 | 2.49559300 | 0.97572800 |
| C | -9.57150100 | 0.71271100 | 1.23896600 |
| H | -10.49424800 | 1.24498400 | 1.44878200 |
| C | -8.42060600 | -1.40970500 | 0.97810000 |
| H | -8.41486400 | -2.49568400 | 0.97760300 |
| C | -9.57138700 | -0.71279000 | 1.23950800 |
| H | -10.49404700 | -1.24505100 | 1.44973100 |
| N | -2.38546100 | 3.53543100 | -0.61267200 |
| N | -2.38535000 | -3.53563400 | -0.61151800 |
| C | -2.38533700 | 4.96570500 | -0.91295200 |
| H | -1.94628300 | 5.55401400 | -0.09769800 |

| | | | |
|---|---|---|---|
| H | -1.82898200 | 5.16960500 | -1.83410100 |
| H | -3.41673400 | 5.28048600 | -1.06028800 |
| C | -2.38525000 | -4.96593300 | -0.91166800 |
| H | -1.82949800 | -5.16985600 | -1.83317900 |
| H | -1.94554200 | -5.55410200 | -0.09666500 |
| H | -3.41669600 | -5.28088300 | -1.05828000 |
| F | -4.08437300 | 3.47682300 | 1.08085100 |
| F | -4.69759800 | 3.31324600 | -1.11971100 |
| F | -4.08377900 | -3.47637400 | 1.08256500 |
| F | -4.69763600 | -3.31391900 | -1.11789700 |
| B | -3.72873200 | 2.99404100 | -0.17515700 |
| B | -3.72850000 | -2.99416700 | -0.17375600 |

## 5. Absorption spectra

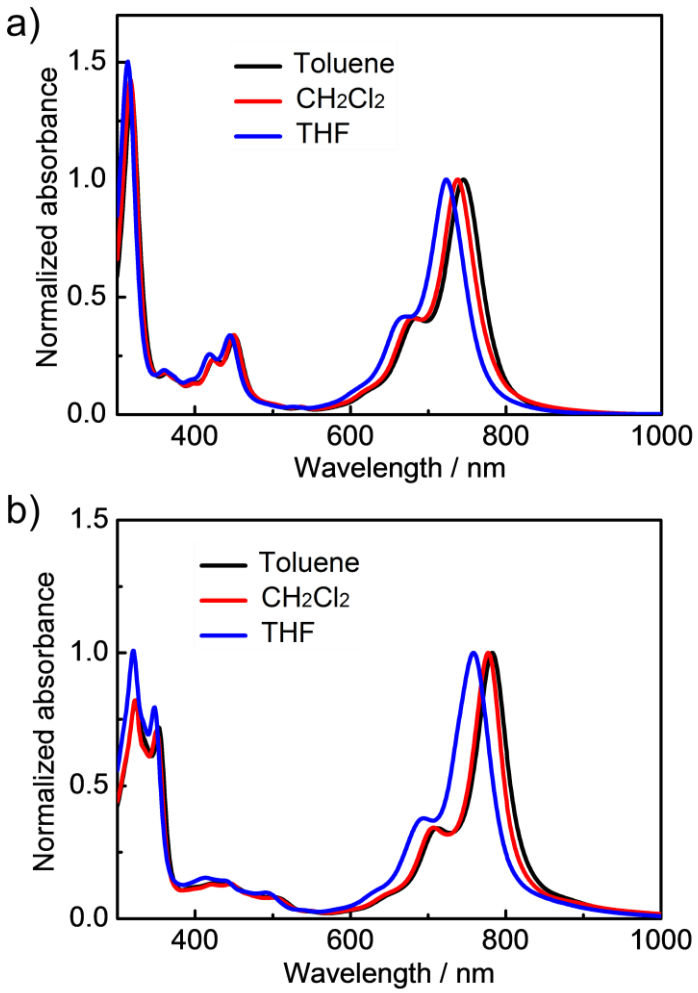


**Figure S5**. UV/Vis absorption spectra of a) **5a** and b) **5b** in various solutions.

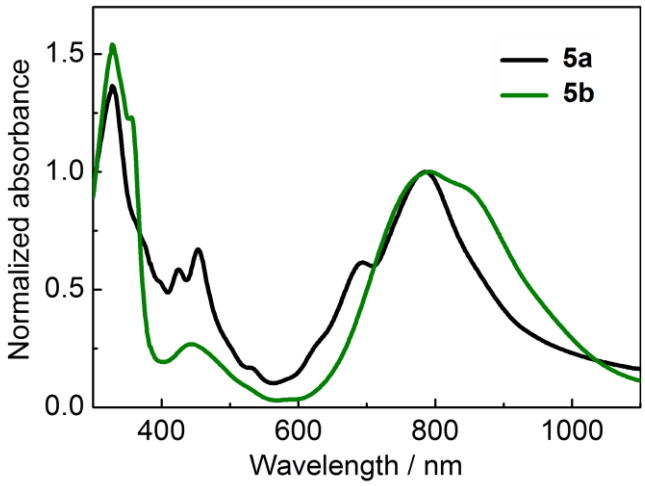


**Figure S6**. UV/Vis absorption spectra of **5a** and **5b** in thin films. The films show the broad and red-shifted absorptions with the $\lambda_{abs}$ of ca. 785 nm for them.

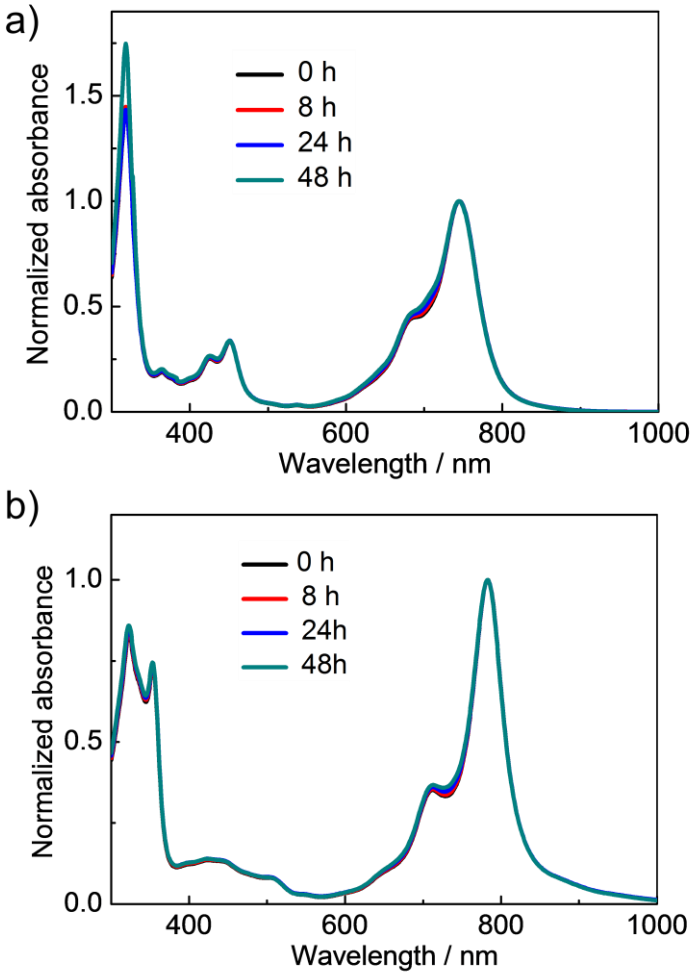


**Figure S7**. UV/Vis absorption spectra of a) **5a** and b) **5b** in toluene with the solutions left at ambient conditions. No change of the spectra suggests that **5a** and **5b** are very stable toward air and moisture.

## 6. Theoretical calculations

Density functional theory (DFT) calculations at the B3LYP/6-31G(d,p) level of theory were performed on **5a-Me**, **5b-Me**, **5a-CC** and **5b-CC**. To assign the absorption bands observed in the UV/Vis spectra of **5a** and **5b**, time-dependent DFT calculations were performed on **5a-Me** and **5b-Me** using Gaussian 09 program at the B3LYP/6-31G(d,p) level of theory.

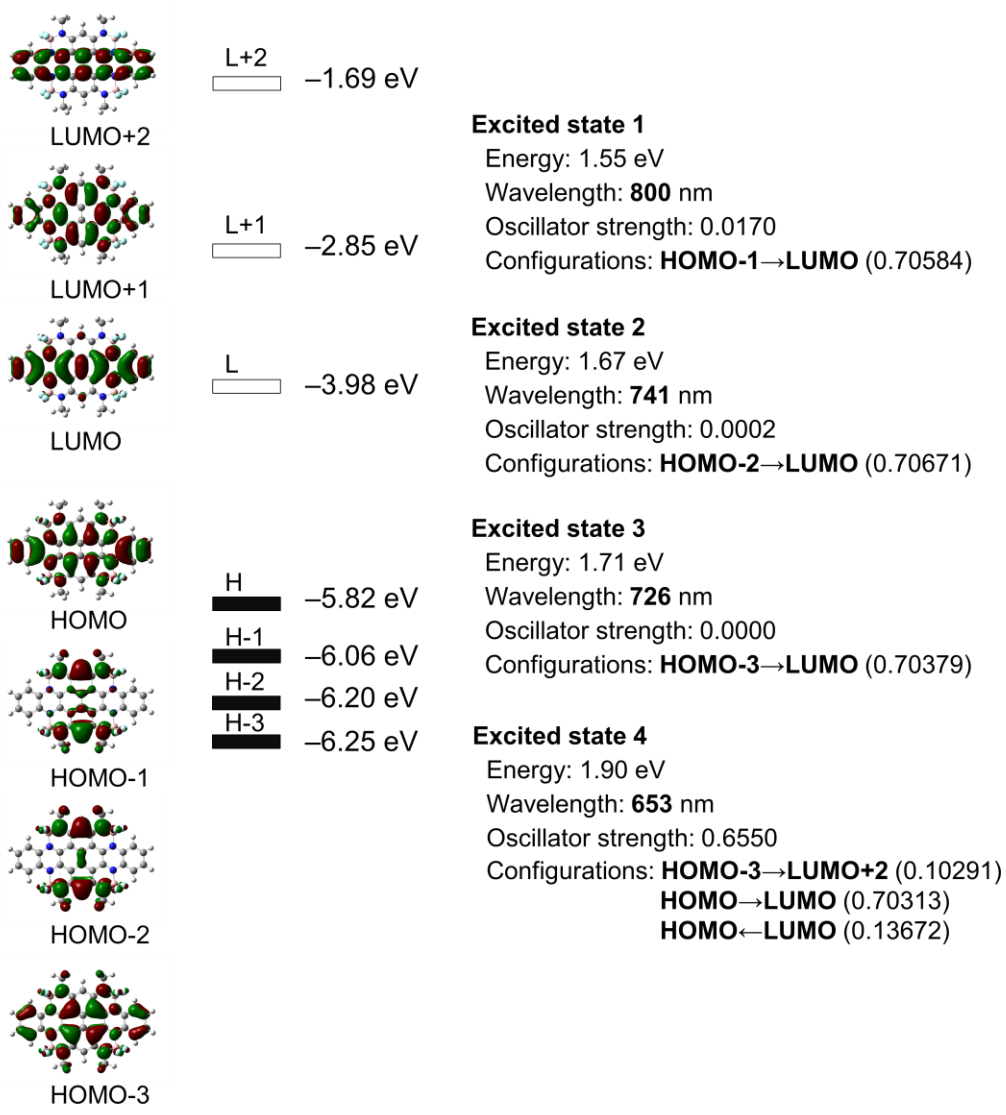


**Figure S8.** The molecular orbitals, energy levels, excitation energies and oscillator strengths of **5a-Me**, based on the TD-DFT (B3LYP/6-31G(d,p)) calculation.

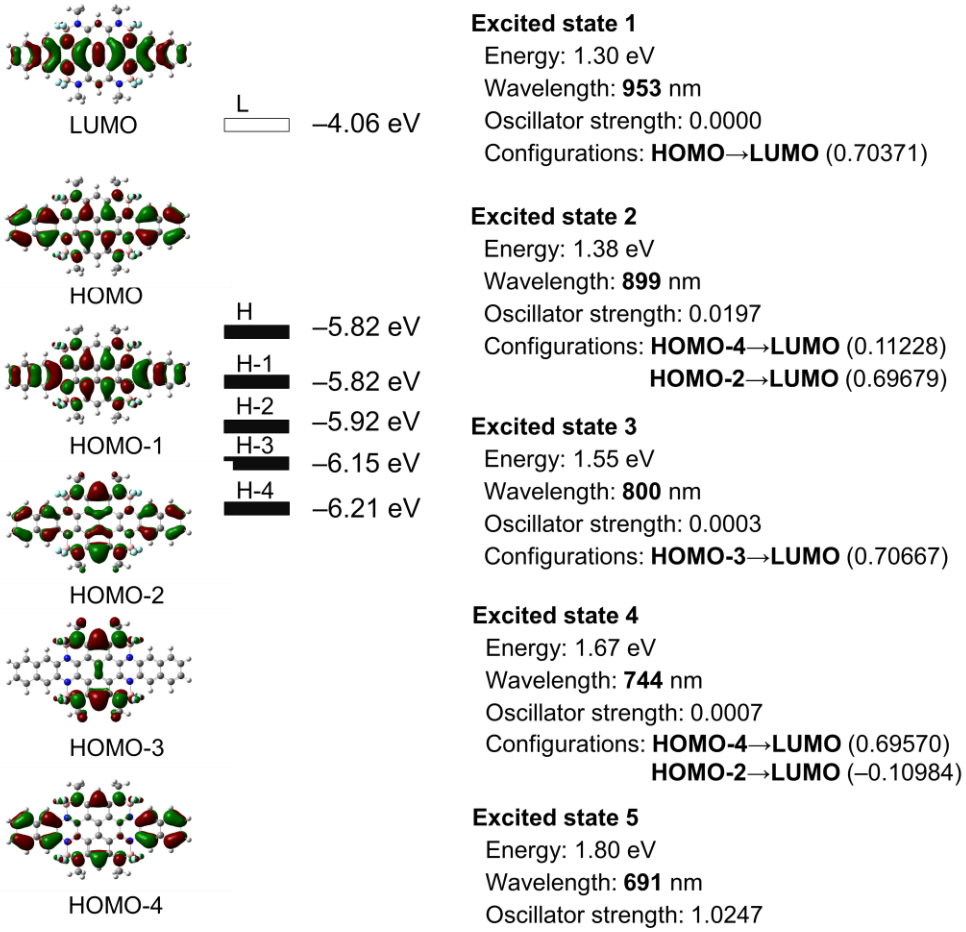


**Figure S9.** The molecular orbitals, energy levels, excitation energies and oscillator strengths of **5b-Me**, based on the TD-DFT (B3LYP/6-31G(d,p)) calculation.

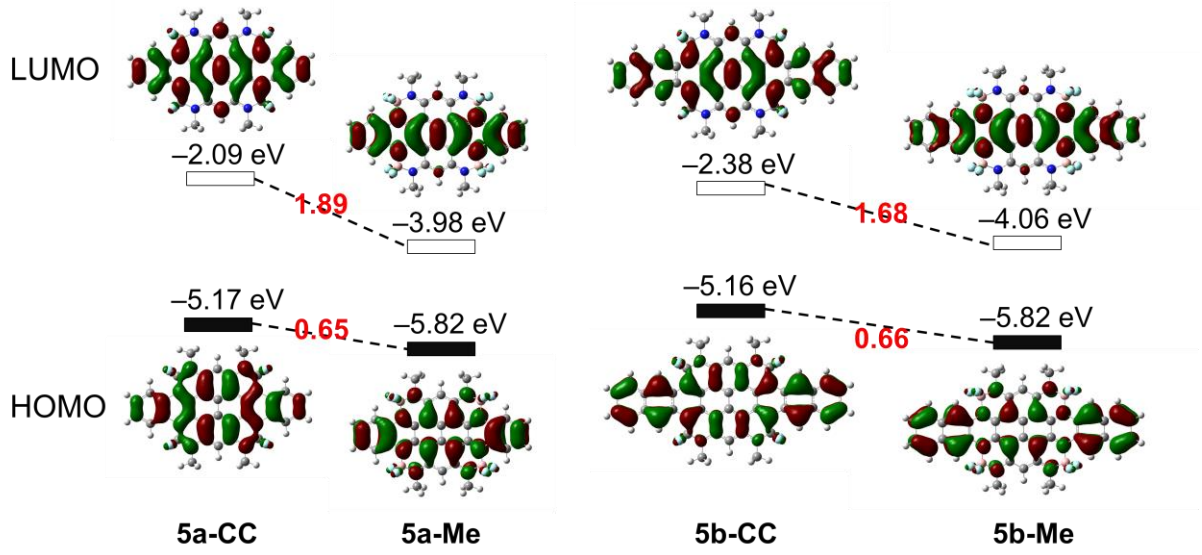


**Figure S10.** The molecular orbitals and energy levels of **5a-Me**, **5b-Me**, **5a-CC** and **5b-CC**, based on the DFT (B3LYP/6-31G(d,p)) calculation.

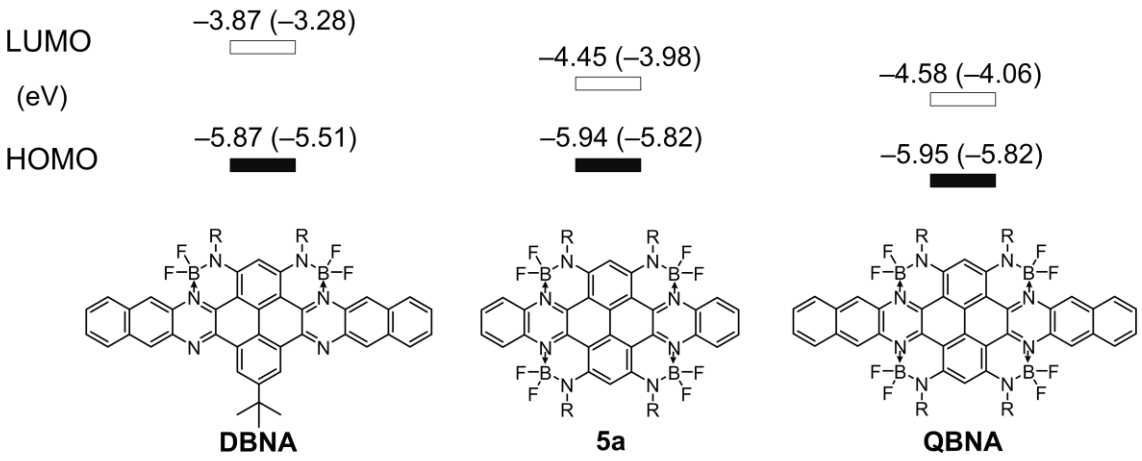


**Figure S11.** The experimental $E_{LUMO}$ and $E_{HOMO}$ accompanying with the theoretical values of **DBNA**, **5a** and **QBNA**.

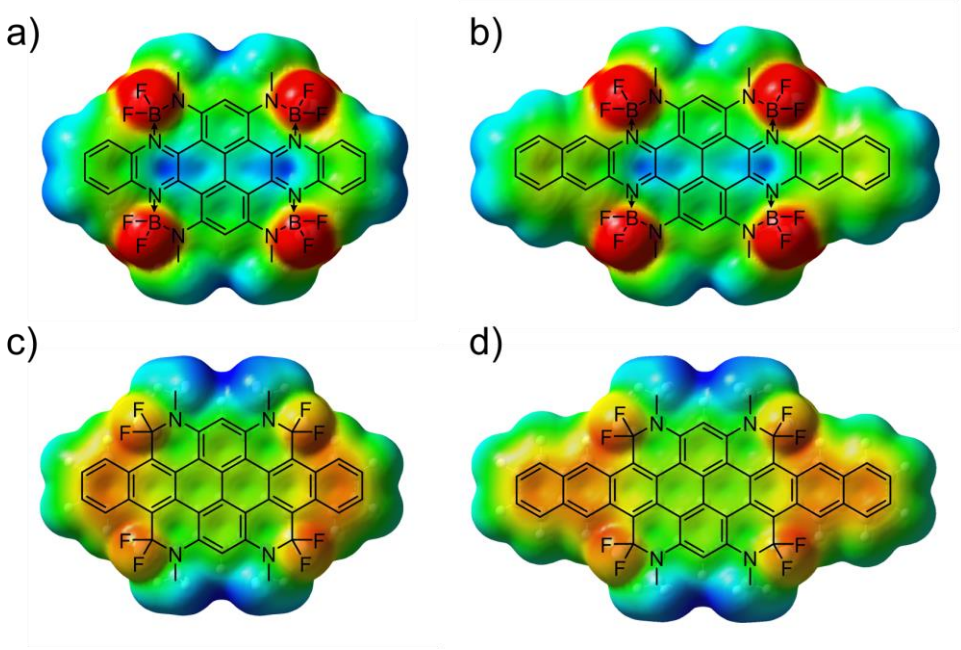


**Figure S12.** Electrostatic potential surface (EPS) maps at the 0.0004 electron density of **5a-Me**, **5b-Me**, **5a-CC** and **5b-CC**.

After replacing the C−C bonds by the B←N units, the electronic energy levels of conjugated polyarenes, especially the LUMO levels, are significantly decreased. Moreover, while the π-frameworks in **5a-CC** and **5b-CC** are electronically negative, the π-frameworks in **5a-Me** and **5b-Me** are electronically positive. These results demonstrate the electron-withdrawing B←N unit can significantly enhance the electron affinity of π-systems.

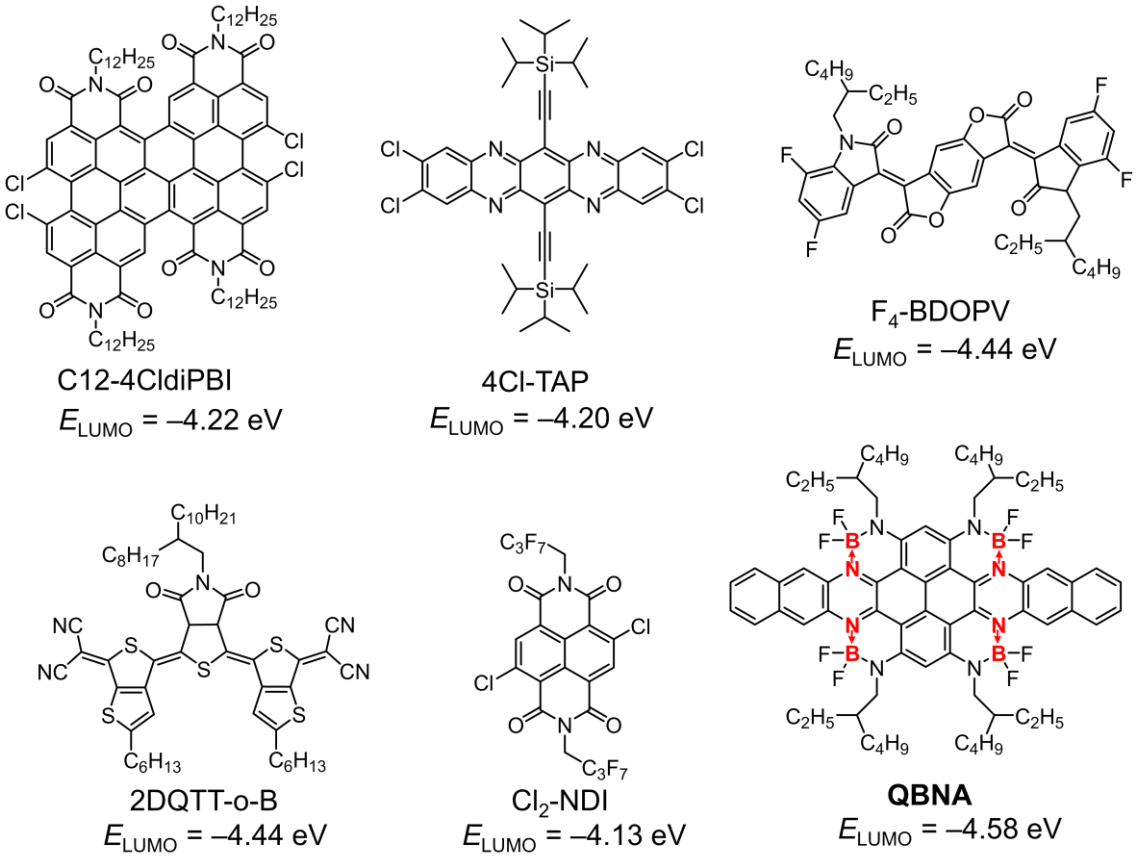


**Figure S13.** Chemical structures and LUMO energy levels of chlorinated aromatic diimides (C12-4CldiPBI and $Cl_2$-NDI),[2,3] chlorinated tetraazapentacene (4Cl-TAP),[4] fluorinated benzodifurandione-based oligo(p-phenylenevinylene) ($F_4$-BDOPV),[5] cyano-containing quinoidal terthiophenes (2DQTT-o-B)[6] and **QBNA**.

To further demonstrate the high electron affinity of **QBNA**, we compare its LUMO level with those of the reported high-performance n-type organic semiconductors. The experimental LUMO levels are calculated based on $E_{LUMO} = -(4.80 + E_{1/2}^{red1})$ eV. As shown in Figure S13, the $E_{LUMO}$ of these n-type organic semiconductors are ca. −4.2~−4.5 eV, which are quite comparable to that (−4.58 eV) of **QBNA**. These comparisons clearly verify the extremely high electron affinity of quadruply B←N-fused dibenzo-azaacene.

**7. SC-OFET device fabrications and characterizations**

Single-crystal organic field-effect transistors (SC-OFETs) were fabricated with a bottom-gate/ top-contact (BGTC) configuration. The substrates with silicon wafer covered with 300 nm $SiO_2$ were cleaned with double-distilled water, piranha solution ($H_2SO_4$:$H_2O_2$ = 7:3), double-distilled water, and isopropanol and then dried under a high-purity nitrogen flow. The modification of $SiO_2$/Si wafers was carried out using octadecyltrichlorosilane (OTS) with the vapor-deposition method: the cleaned wafers were cleaned with oxygen plasma (10 min, 100W), then were dried under vacuum at 90 ℃ for 1.5 h. After decreasing the temperature to 60 ℃, a small drop of OTS was dropped onto the $SiO_2$/Si wafers. This system was then heated at 120 ℃ for 2 h under vacuum. The OTS modified $SiO_2$/Si wafers were cleaned with n-hexane, chloroform and isopropyl alcohol, and finally were dried with high-purity nitrogen flow.

Single-crystal microwires of **QBNA** were prepared in typical growth conditions through drop-casting of its toluene solution (1 mg/mL) onto the OTS modified $SiO_2$/Si substrates in a sealed bottle at 25 ℃. Single-crystal microwires gradually appeared on the substrates with the solution evaporation. Then the SC-OFET devices were fabricated with the organic ribbon mask method. An individual micrometer organic nanowire made in advance was first put on a microwire perpendicularly to the growth direction under a high-resolution microscopy (magnification at x400−1000). A layer of 20 nm Au was then deposited on the masked microwire as the source and drain electrodes. Finally, the organic nanowires were removed and a device with two electrodes was obtained. All electrical characteristics of the devices were measured at room temperature in air using a semiconductor parameter analyser (Keithley 4200 SCS) and a micromanipulator 6150 probe station. The mobility was extracted from the saturation region by using the equation of $I_{DS} = (W/2L)C_i\mu(V_G-V_T)^2$, where $I_{DS}$ is the drain-source current, μ is the field-effect mobility, $C_i$ is the capacitance per unit area of the gate dielectric layer, $V_G$ and $V_T$ are the gate voltage and threshold voltage, L and W are the channel length and width basing on an individual microwire in SC-OFET devices, respectively.

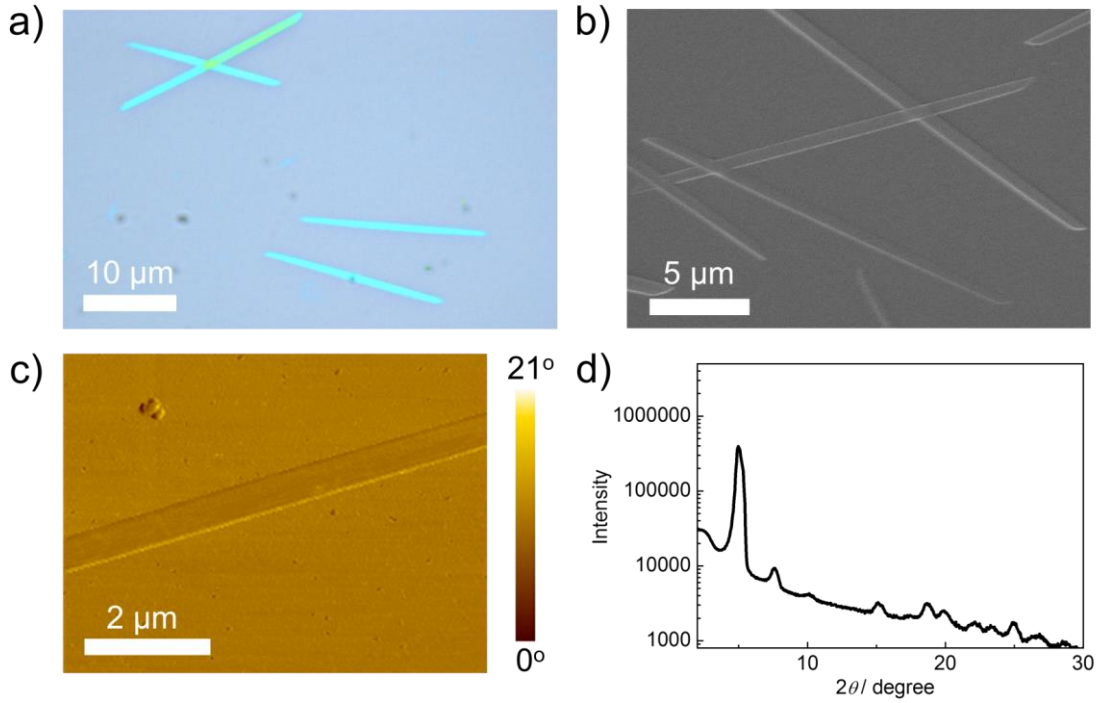


**Figure S14.** a−c) Optical microscopy, SEM and AFM images of the single-crystal microwires and d) X-ray diffraction pattern of the microwires of **5b**.

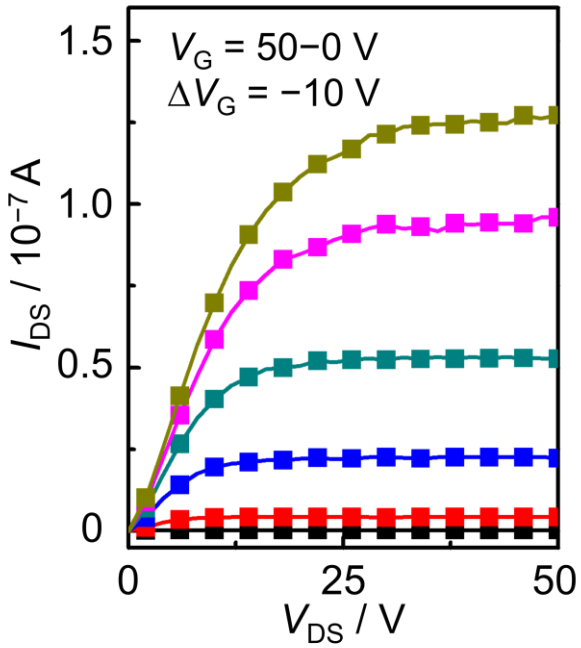


**Figure S15.** Output curves of the SC-OFET device based on **5b**.

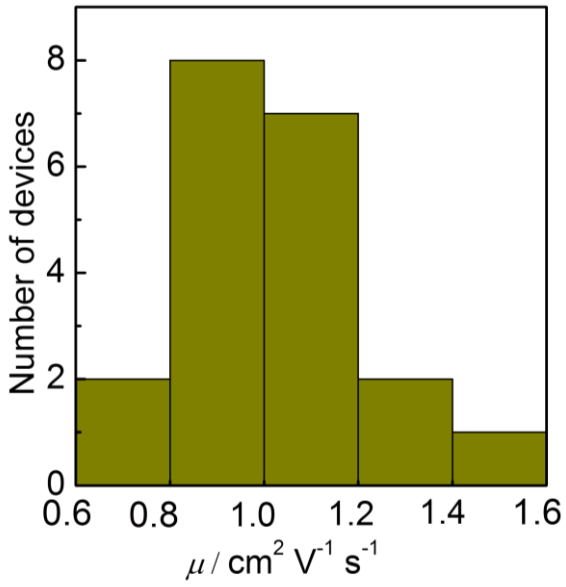


**Figure S16.** The electron mobility distribution of twenty SC-OFET devices based on **5b**.

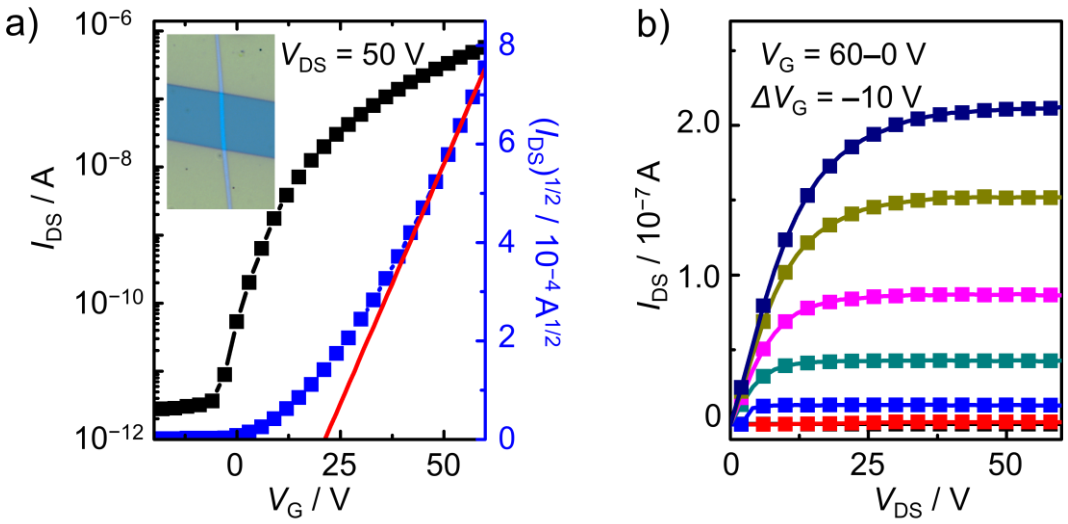


**Figure S17.** Transfer and output curves of the SC-OFET device based on the microwires from the solution of **5b** in *o*-xylene.

We have optimized the device fabrication conditions of **5b**. The solutions of **5b** in toluene, *o*-xylene, $CHCl_3$ and chlorobenzene were used to grow its micrometer-sized single crystals. We could obtain some single-crystal microwires that are suitable for SC-OFETs from its toluene and *o*-xylene solutions. As shown in Figure S15, the SC-OFET device based on the microwires from the solution of **5b** in *o*-xylene exhibits the unipolar n-type behavior with an electron mobility of 1.25 $cm^2\ V^{-1}\ s^{-1}$, an on/off current ratio of $10^5$–$10^6$ and a threshold voltage of 21 V.

## 8. $^{1}$H NMR and $^{13}$C NMR spectra

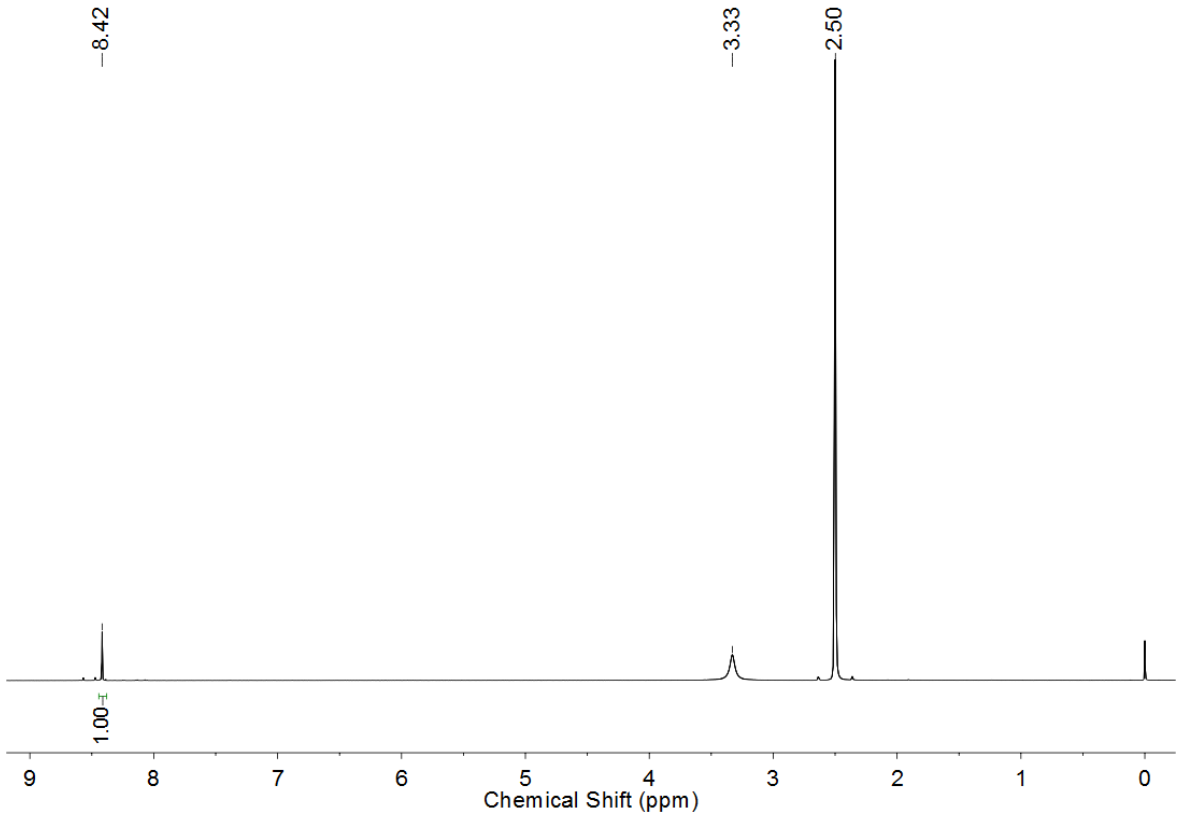


**Figure S18**. $^{1}$H NMR spectrum of **2** in *d*-DMSO.

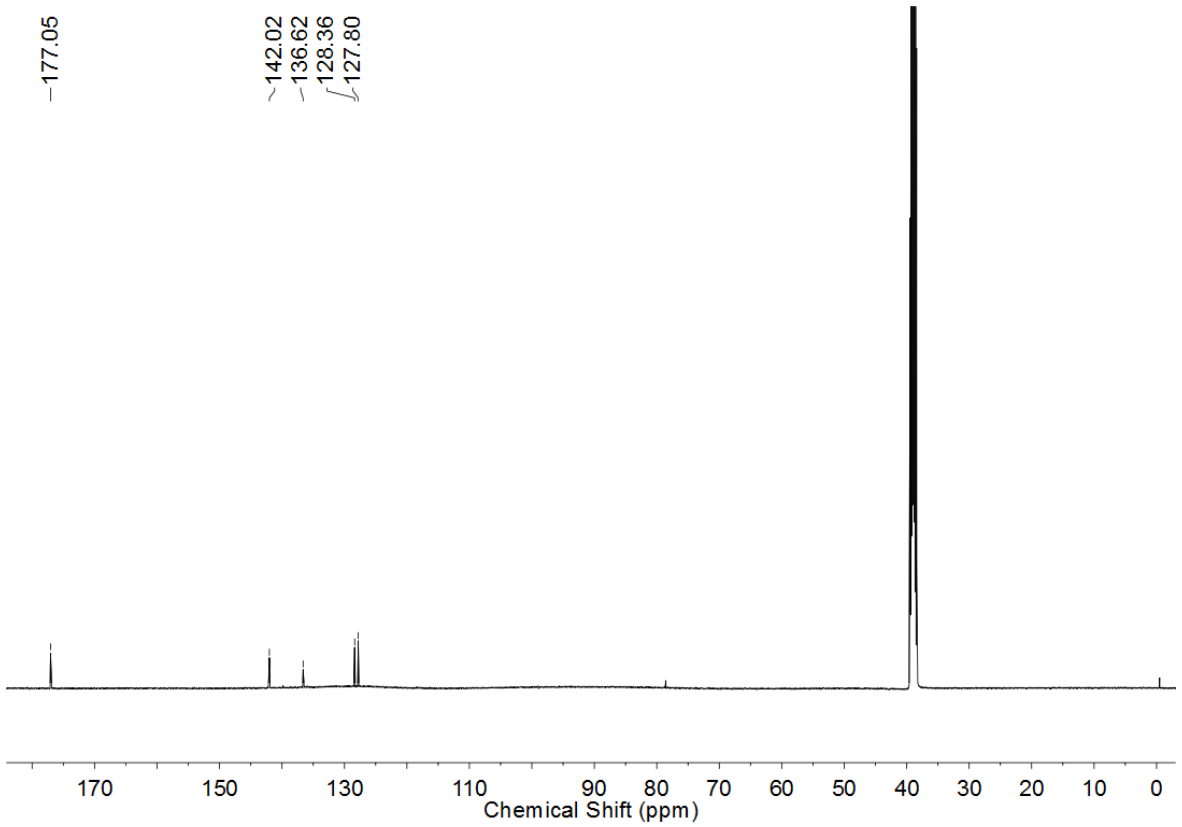


**Figure S19**. $^{13}$C NMR spectrum of **2** in *d*-DMSO.

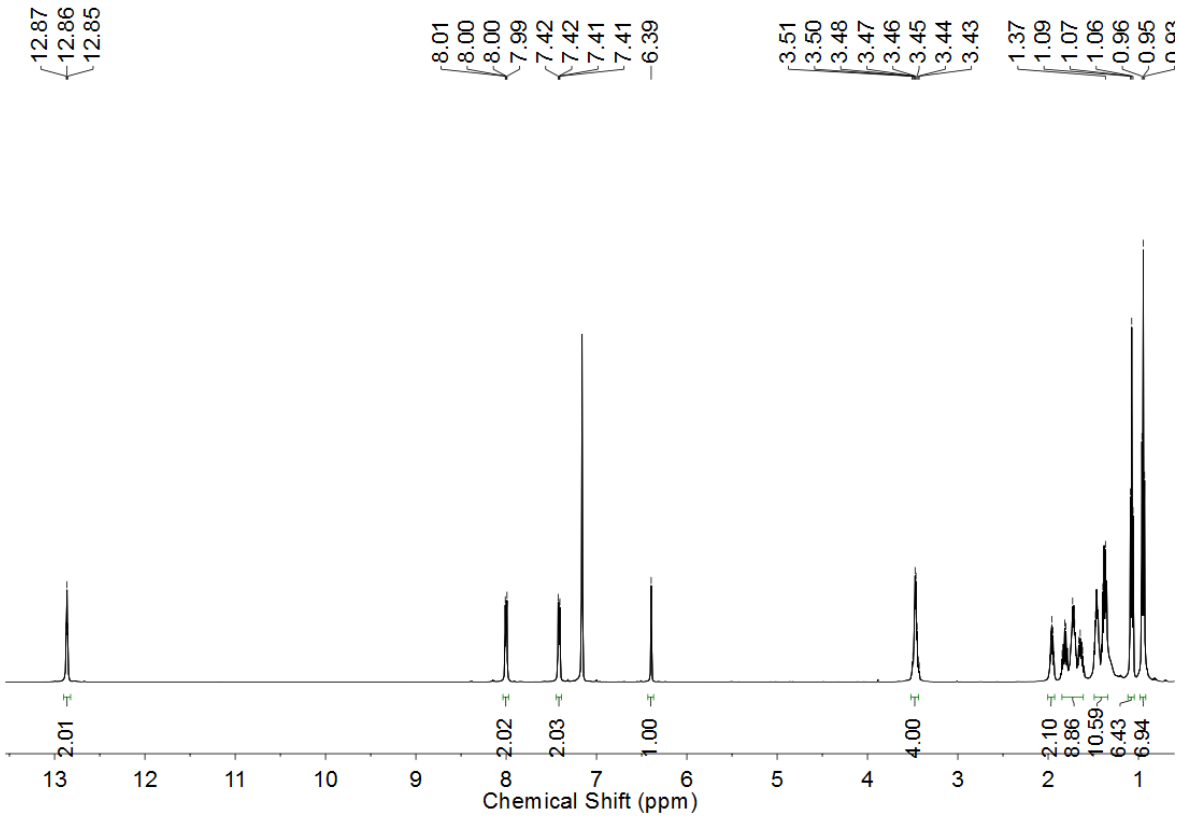


**Figure S20**. $^{1}$H NMR spectrum of **4a** in $C_6D_6$.

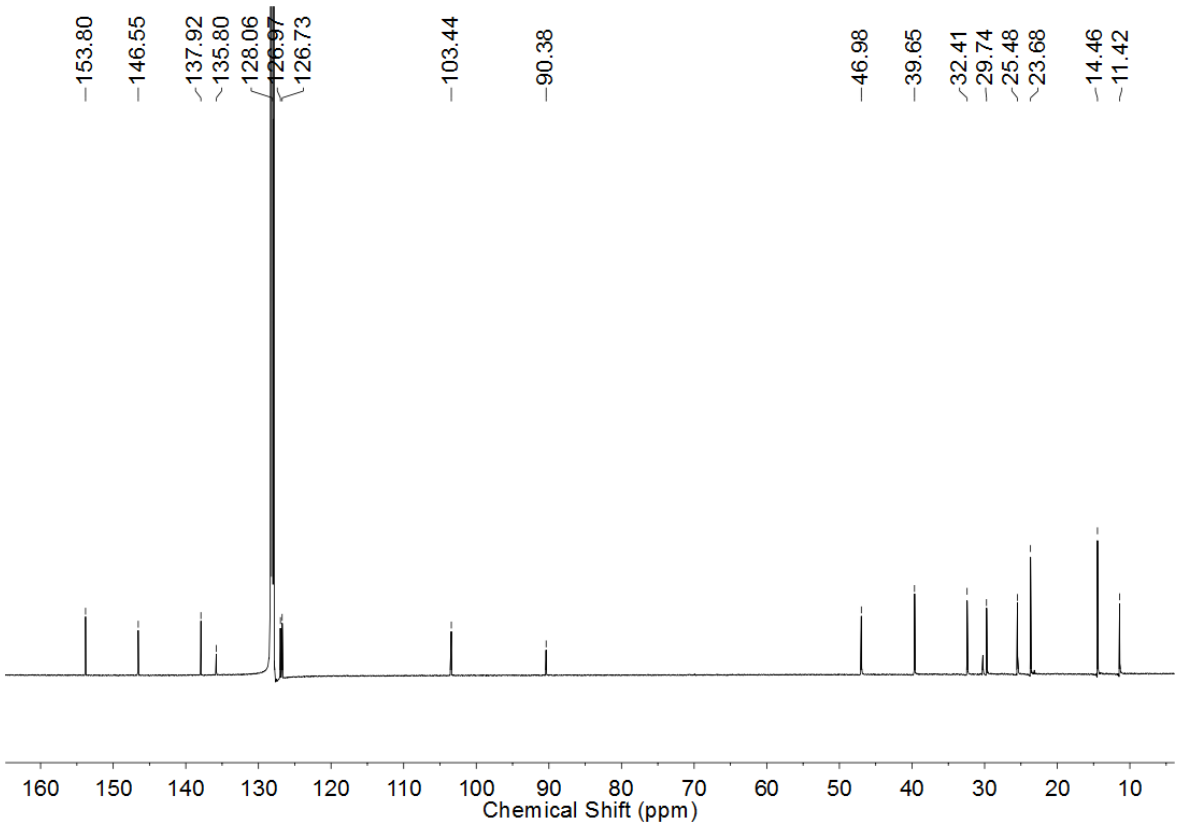


**Figure S21**. $^{13}$C NMR spectrum of **4a** in $C_6D_6$.

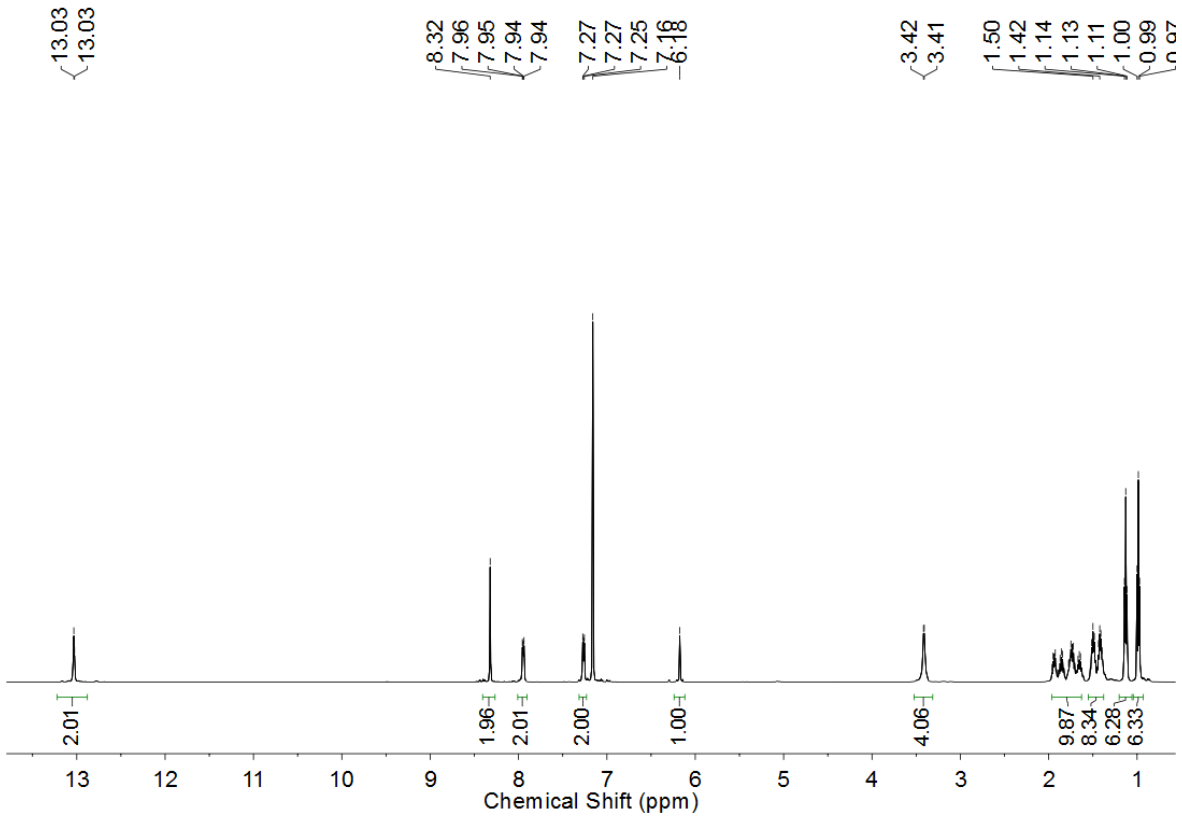


**Figure S22**. $^{1}$H NMR spectrum of **4b** in $C_6D_6$.

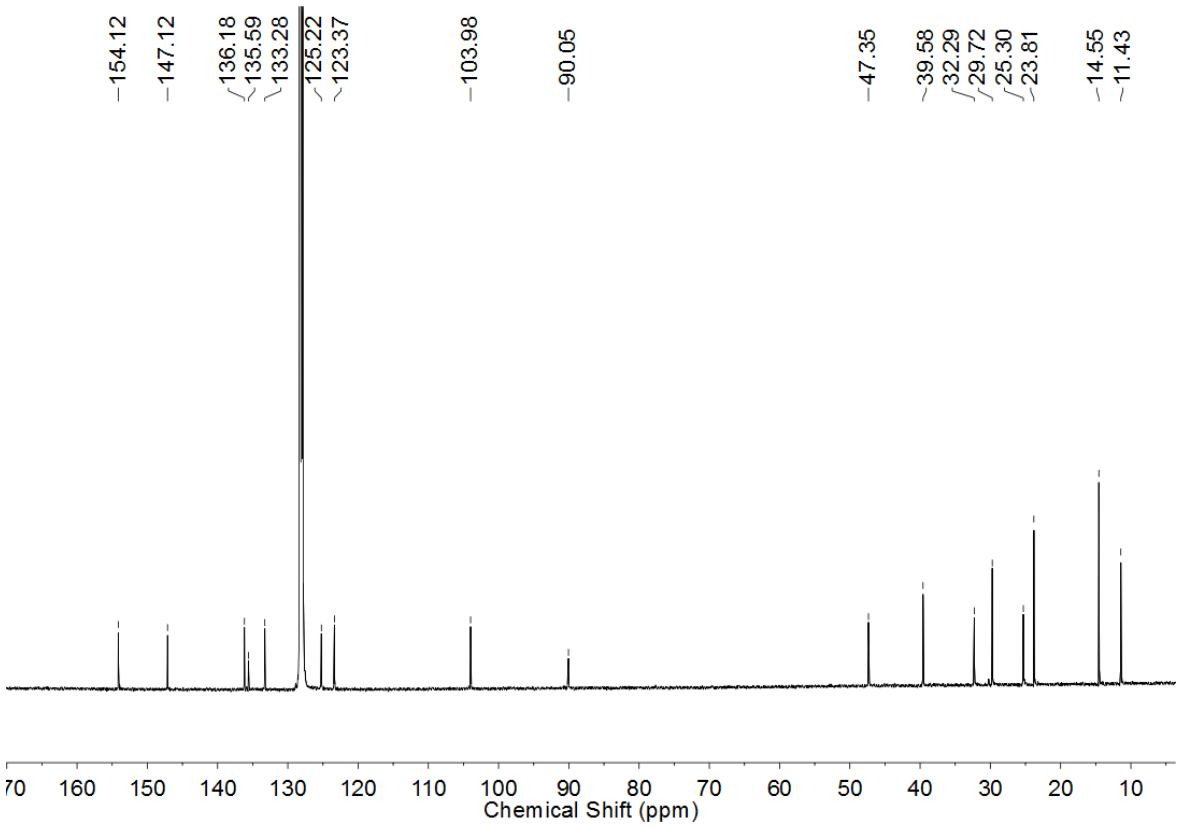


**Figure S23**. $^{13}$C NMR spectrum of **4b** in $C_6D_6$.

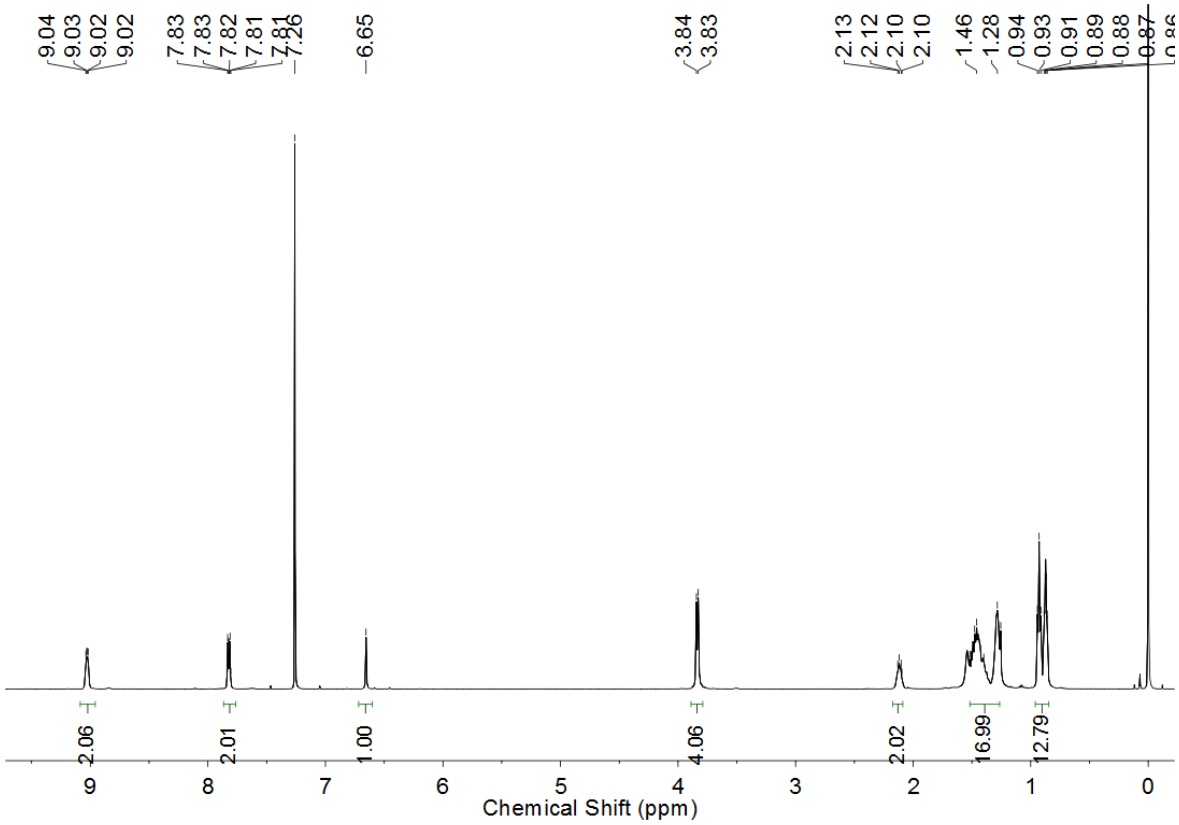


**Figure S24**. $^{1}$H NMR spectrum of **5a** in $CDCl_3$.

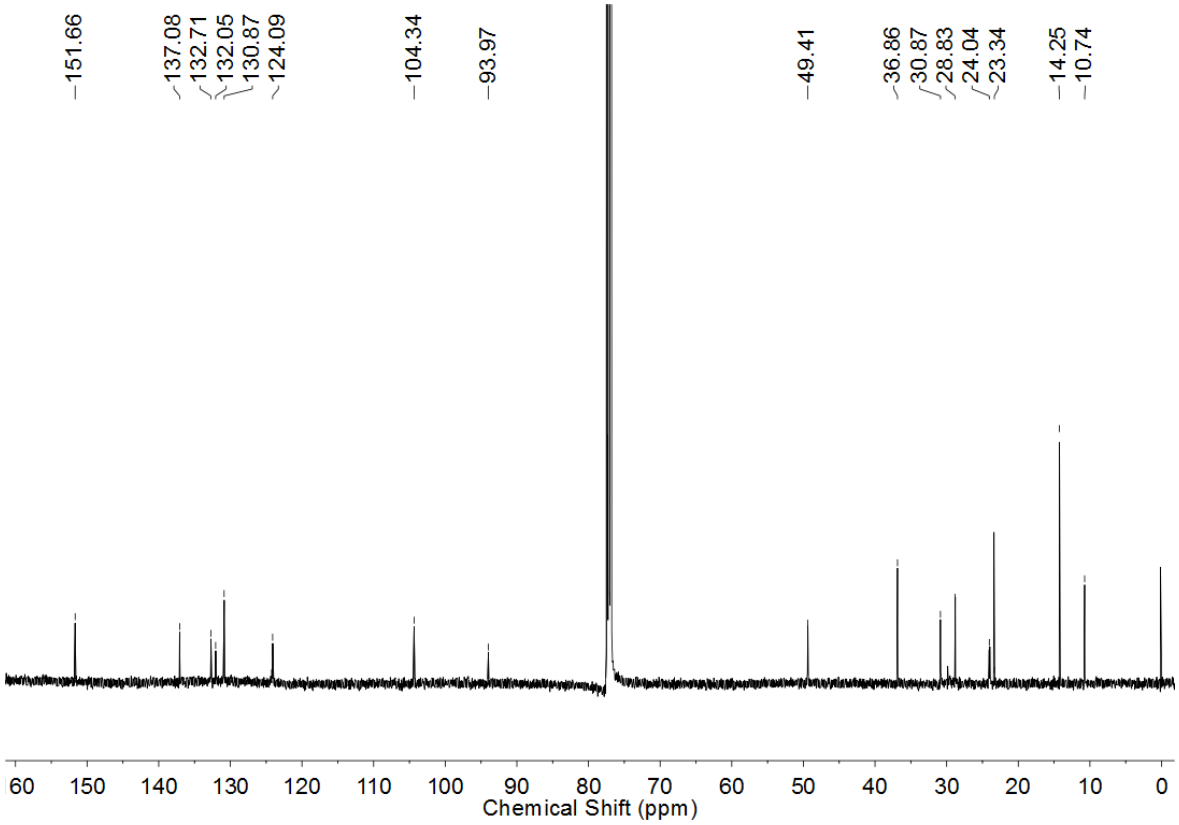


**Figure S25**. $^{13}$C NMR spectrum of **5a** in $CDCl_3$.

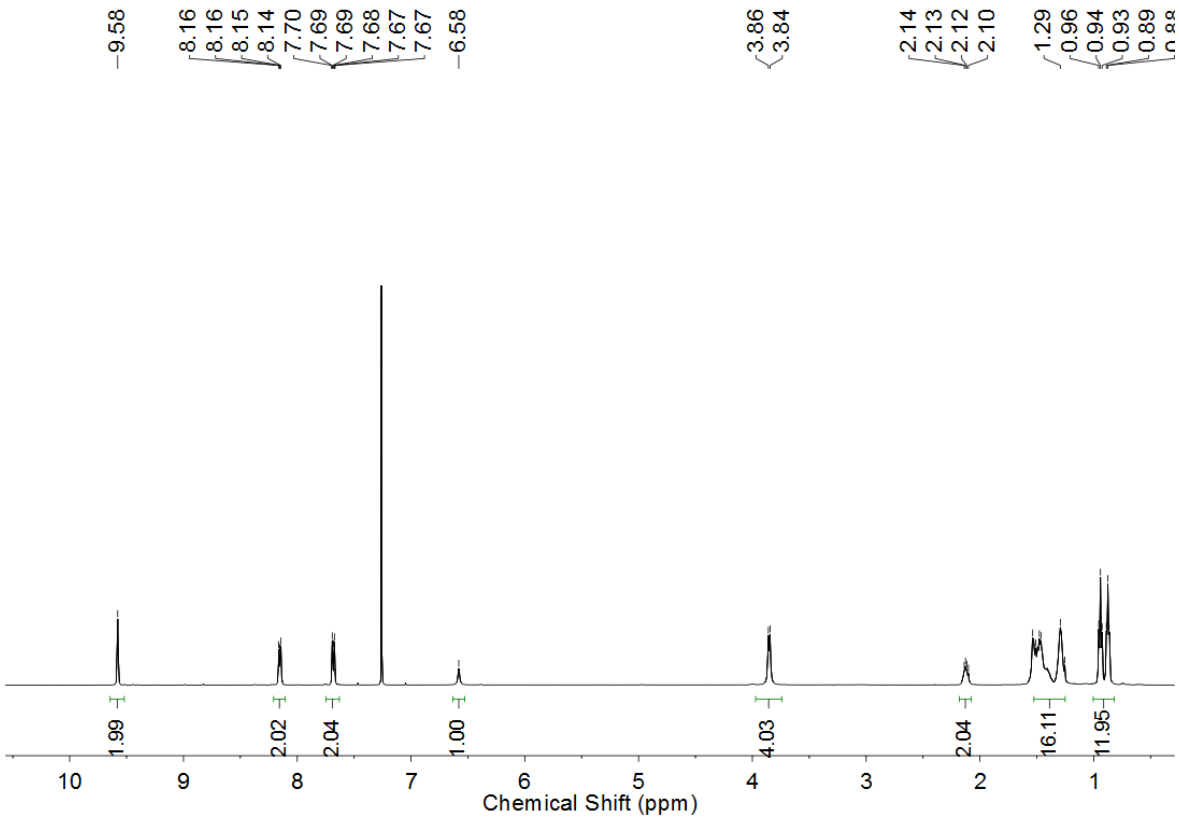


**Figure S26**. $^{1}$H NMR spectrum of **5b** in $CDCl_3$.

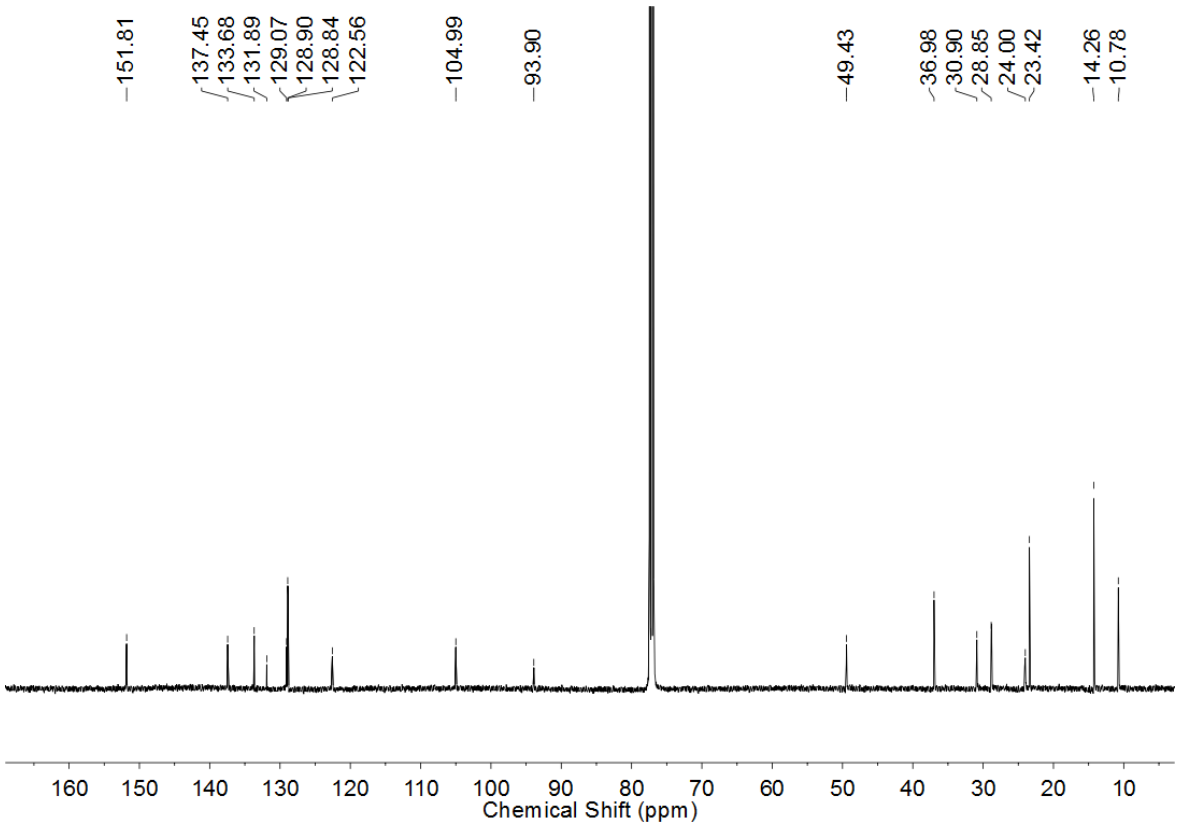


**Figure S27**. $^{13}$C NMR spectrum of **5b** in $CDCl_3$.

## 9. Reference

(1) Gaussian 09 (Revision A.02), Frisch, M. J.; Trucks, G. W.; Schlegel, H. B.; Scuseria, G.E.; Robb, M. A.; Cheeseman, J. R.; Scalmani, G.; Barone, V.; Mennucci, B.; Petersson, G. A.; Nakatsuji, H.; Caricato, M.; Li, X.; Hratchian, H. P.; Izmaylov, A. F.; Bloino, J.; Zheng, G.; Sonnenberg, J. L.; Hada, M.; Ehara, M.; Toyota, K.; Fukuda, R.; Hasegawa, J.; Ishida, M.; Nakajima, T.; Honda, Y.; Kitao, O.; Nakai, H.; Vreven, T.; Montgomery, Jr., J. A.; Peralta, J. E.; Ogliaro, F.; Bearpark, M.; Heyd, J. J.; Brothers, E.; Kudin, K. N.;Staroverov, V. N.; Kobayashi, R.; Normand, J.; Raghavachari, K.; Rendell, A.; Burant, J. C.; Iyengar, S. S.; Tomasi, J.; Cossi, M.; Rega, N.; Millam, J. M.; Klene, M.; Knox, J. E.; Cross, J. B.; Bakken, V.; Adamo, C.; Jaramillo, J.; Gomperts, R.; Stratmann, R. E.; Yazyev, O.; Austin, A. J.; Cammi, R.; Pomelli, C.; Ochterski, J. W.; Martin, R. L.; Morokuma, K.; Zakrzewski, V. G.; Voth, G. A.; Salvador, P.; Dannenberg, J. J.; Dapprich,S.; Daniels, A. D.; Farkas, O.; Foresman, J. B.; Ortiz, J. V.; Cioslowski, J.; Fox, D. J. Gaussian, Inc., Wallingford CT, **2009**.

(2) Lv, A.; Puniredd, S. R.; Zhang, J.; Li, Z.; Zhu, H.; Jiang, W.; Dong, H.; He, Y.; Jiang, L.; Li, Y.; Pisula, W.; Meng, Q.; Hu, W.; Wang, Z. *Adv. Mater*. **2012**, *24*, 2626−2630.

(3) Oh, J. H.; Suraru, S.-L.; Lee, W.-Y.; Könemann, M.; Höffken, H. W.; Röger, C.; Schmidt, R.; Chung, Y.; Chen, W.-C.; Würthner, F.; Bao, Z. *Adv. Funct. Mater*. **2010**, *20*, 2148−2156.

(4) Chu, M.; Fan, J.-X.; Yang, S.; Liu, D.; Ng, C. F.; Dong, H.; Ren, A.-M.; Miao, Q. *Adv. Mater*. **2018**, *30*, 1803467.

(5) Dou, J.-H.; Zheng, Y.-Q.; Yao, Z.-F. Yu, Z.-A.; Lei, T.; Shen, X.; Luo, X.-Y.; Sun, J.; Zhang, S.-D.; Ding, Y.-F.; Han, G.; Yi, Y.; Wang, J.-Y.; Pei, J. *J. Am. Chem. Soc*. **2015**, *137*, 15947−15956.

(6) Zhang, C.; Zang, Y.; Zhang, F.; Diao, Y.; McNeill, C. R.; Di, C.-A.; Zhu, X.; Zhu, D. *Adv. Mater*. **2016**, *28*, 8456−8462.